Quantitative Structures and Thermal Properties of Birch Lignins after Ionic Liquid Pretreatment

Jia-Long Wen,[†] Shao-Long Sun,[†] Bai-Liang Xue,[†] and Run-Cang Sun*,[†,‡]

[†]Beijing Key Laboratory of Lignocellulosic Chemistry, Beijing Forestry University,Beijing, China
[‡]State Key Laboratory of Pulp and Paper Engineering, South China University of Technology, Guangzhou, China

ⓢ *Supporting Information*

ABSTRACT: The use of ionic liquid (IL) in biomass pretreatment has received considerable attention recently because of its effectiveness in decreasing biomass recalcitrance to subsequent enzymatic hydrolysis. To understand the structural changes of lignin after pretreatment and enzymatic hydrolysis process, ionic liquid lignin (ILL) and subsequent residual lignin (RL) were sequentially isolated from ball-milled birch wood. The quantitative structural features of ILL and RL were compared with the corresponding cellulolytic enzyme lignin (CEL) by nondestructive techniques (e.g., FTIR, GPC, quantitative ^{13}C, 2D and ^{31}P NMR). The IL pretreatment caused structural modifications of lignin (cleavage of β-O-4 ether linkages and formation of condensed structures). In addition, lignin fragments with lower S/G ratios were initially extracted, whereas the subsequently extracted lignin is rich in syringyl unit. Moreover, the maximum decomposition temperature (T_M) was increased in the order ILL < RL < CEL, which was related to the corresponding β-O-4 ether linkage content and molecular weight (M_w). On the basis of the results observed, a possible separation mechanism of IL lignin was proposed.

KEYWORDS: ionic liquid lignin, nuclear magnetic resonance (NMR), β-O-4, molecular weight, thermal properties

■ INTRODUCTION

Lignin is an amorphous and aromatic polymer that acts as the essential glue which links hemicelluloses and cellulose together to give rigidity to plants. In general, lignin is deemed to be constructed from three basic monolignols (p-coumaryl, coniferyl, and sinapyl alcohols), which form various interunit bonds, such as several types of ether (e.g., β-O-4, α-O-4, and 4-O-5) and carbon−carbon (e.g., β-β, β-5, and 5-5) linkages under the conditions of laccases and peroxidases.[1] Besides the linkages within lignin itself, lignin is known to bind physically or chemically to cellulose and hemicelluloses by covalent bonds such as benzyl−ether, benzyl−ester, and phenyl−glycoside bonds, forming lignin−carbohydrate complexes (LCC) in plant cell walls.[2] The complex structure of the lignin−hemicelluloses network is the major reason for the difficulty in isolating pure lignin in an unaltered form.

For decades, a lot of work was devoted to understanding the structural features of native lignin macromolecule from the plant cell wall. Prior to structural analysis of lignin, separating lignin in a relatively unaltered state should be achieved. Motivated by the aim of isolating native lignin from cell wall, several representative methods were proposed. For instance, milled wood lignin (MWL) was first proposed by Björkman.[3] Afterward, cellulolytic enzyme lignin (CEL), which utilizes cellulolytic enzymes to remove most of the carbohydrate fractions prior to aqueous dioxane extraction of ball-milled wood meal, had been presented by Chang and his colleagues.[4] A novel procedure using the combination of enzymatic and mild acidolysis, named enzymatic mild acidolysis lignin (EMAL), has been proposed by Wu and Argyropoulos.[5] All of these methods could be used to investigate the native lignin from plant cell wall.

Along with native lignin isolation progress, analytical methods for lignin characterization were also significantly improved, such as nitrobenzene oxidation (NBO),[6] thioacidolysis (TA),[7] and derivatization followed by reductive cleavage (DFRC).[8] Wet chemistry methods can be very precise for specific functional groups and structural moieties. However, each chemical method gives limited information (mainly noncondensed lignin units) and is not able to provide a general picture of the entire lignin structure. In contrast, quantitative ^{13}C NMR nuclear magnetic resonance (NMR) has the advantages of the analysis of the whole lignin structure and direct detection of lignin moieties.[9−11] Especially, quantitative ^{13}C NMR and two-dimensional heteronuclear single-quantum coherence (2D-HSQC) have been developed to quantify the lignin structures and LCC linkages.[12−14]

Recently, ionic liquids (ILs) have attracted significant attention as a promising green solvent with environmental friendliness in the field of lignocellulosic biomass utilization. Many ILs are able to dissolve wood biomass and its major components, cellulose, hemicelluloses, and lignin.[15] It has been demonstrated that IL pretreatment facilitates the "delignification process" and significantly increases the enzymatic hydrolysis efficiency of pretreated biomass.[16,17] However, its commercialization is hindered by the high cost of ILs. The efficient recycling of ILs, as well as the valorization of the lignin byproducts of biomass deconstruction, is of prime importance to the large-scale success of IL pretreatment processes.[18] To achieve the high-value utilization of lignocellulosic biomass,

isolation and chemical conversion of the isolated component are urgently needed in the biorefinery. Among numerous ILs, 1-ethyl-3-methylimidazolium acetate, $[C_2min][OAc]$, was demonstrated to effectively extract lignin from wood and to be one of the best solvents for lignocellulosic biomass.[16,17,19,20] A recent paper has demonstrated that the lignin isolated with ionic liquid from poplar wood has similar structural features as compared to the corresponding MWL except for the smaller molecular weight.[21] Torr et al.[22] have investigated the impact of ionic liquid pretreatment on the chemistry and enzymatic digestibility of *Pinus radiata* compression wood and showed that the pretreatment caused some structural modifications to the lignin and polysaccharides. However, to thoroughly understand the $[C_2mim][OAc]$ pretreatment and enzymatic hydrolysis on the structural features of lignin, more representative lignin fractions should be collected and investigated. It is well-known that the structural details of residual lignins (RLs) are of considerable importance in pulp delignification and bleaching studies.[23,24] Therefore, isolation and detailed structural analysis of the RL should be carried out to understand the effects of IL pretreatment on the structures of residual lignin from pretreated lignocellulosic material. More importantly, the well-characterized lignin is beneficial in the development of highly functionalized natural products and chemicals based on the lignin polymer obtained after IL-based biorefinery. Furthermore, the thermal properties should also be investigated if the utilization of lignin involves a thermochemical process, because knowledge of lignin thermal degradation is fundamental for predicting pyrolysis behavior of this feedstock.

In the present study, southwest birch wood, the third fast-growing hardwood species after eucalyptus and poplar in China, was submitted to IL pretreatment and subsequent enzymatic hydrolysis processes. After these processes, two lignin fractions, ionic liquid lignin (ILL) and residual lignin (RL), were successively isolated with high yields and purities. In addition, CEL of birch wood was also isolated for comparison. To thoroughly investigate the structural features of the isolated birch lignins, the lignins were characterized with Fourier transform infrared spectroscopy (FT-IR) and measured by gel permeation chromatography (GPC). Moreover, lignin structural information, such as S/G ratios and the amounts of major substructures (intercoupling bonds, β-O-4, β-β, β-5, etc.), were qualitatively and quantitatively acquired according to quantitative ^{13}C, 2D-HSQC NMR, and ^{31}P NMR spectroscopy. Furthermore, to reveal the relationship between quantitative structural features and thermal properties, thermogravimetric analysis (TGA) was also implemented. The results obtained on the lignins will contribute to the goal of better understanding the structure of lignin and the IL pretreatment processes for native feedstock.

■ MATERIALS AND METHODS

Materials. Hardwood sawdust was prepared from birch wood (*Betula alnoide* Buch.-Ham. ex D. Don, 10 years old, harvested from Yunnan province, China) with a miniature plant mill (Tianjin, China). Then the sawdust was extracted with toluene/ethanol (2:1, v/v) in a Soxhlet instrument for 6 h. The composition of southwest birch was 35.0% glucan, 20.7% xylan, 0.47% arabinan, 7.49% mannan, 1.30% galactan, 23.4% Klason lignin, and 2.00% acid-soluble lignin, which was analyzed by using the methods of Laboratory Analytical Procedure (LAP) of biomass provided by the National Renewable Energy Laboratory (NREL).[25] The extracted birch sawdust (25 g) was then milled using a planetary ball mill (Fritsch, Germany) in a 500 mL ZrO₂ bowl with mixed balls (10 balls of 2 cm diameter and 25 balls of 1 cm

diameter). The milling was conducted for 2 h under a nitrogen atmosphere at 450 rpm.

Celluclast 1.5 L (70 FPU/mL) and Novozyme 188 (240 FPU/mL) were purchased from Novozymes, China. Other reagents of analytical grade were purchased from Sigma-Aldrich unless otherwise stated.

Ionic liquid, 1-ethyl-3-methylimidazolium acetate ($[C_2mim][OAc]$ (≥98%)), was purchased from Lanzhou Institute of Chemical Physics, Lanzhou, China. All chemical reagents used were of analytical grade or best available.

Ionic Liquid Pretreatment and Lignin Isolation. ILL and RL were isolated according to Figure 1. ILL was isolated according to
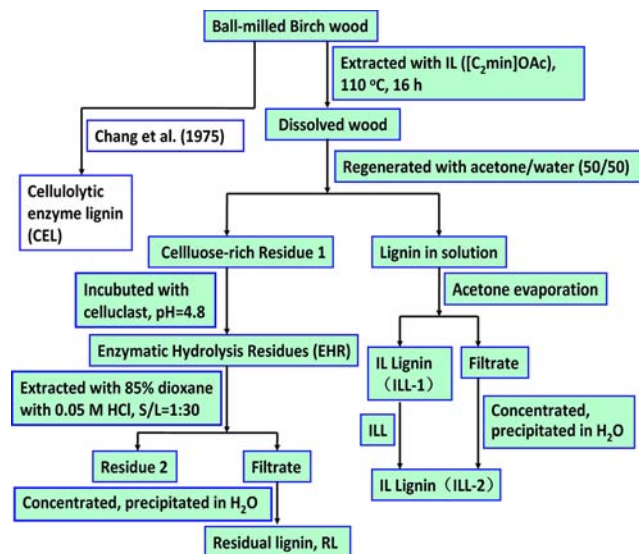

Figure 1. Flowchart of lignin extraction process.

previous literature with minor modifications.[16] The ball-milled birch wood meal (5 g) was added to 1-ethyl-3-methylimidazolium acetate (100 g) in a round-bottom flask (250 mL). The mixture was stirred at 110 °C for 16 h to dissolve the ball-milled meal under nitrogen protection. For regeneration of the dissolved birch wood, the wood/IL solution was poured into a 1000 mL beaker containing 500 mL of acetone/water (1: 1 v/v). The beaker was sealed with parafilm, and the mixture was stirred (1200 rpm/min) at room temperature for 2 h. The regenerated southwest birch wood (cellulosic substance) was filtered through a 0.45 μm filter paper (Whatman, Hangzhou, China) and thoroughly washed with 500 mL of acetone/water (50:50, v/v) to remove the residual ionic liquid. The filtrate was then concentrated under reduced pressure at 40 °C until acetone was removed and insoluble solid ILL was precipitated. After filtration, the crude ILL-1 was collected and washed with distilled water and finally freeze-dried. To obtain more lignin after IL pretreatment, the filtrate was concentrated again and poured into 5 volumes of acidic water (pH 2, HCl), ILL-2 was also obtained by centrifugation at 4000g (Figure 1). The IL was recycled after the evaporation of water from the supernatant after centrifugation, which showed a deep color. Subsequently, the RL from cellulose-rich residue 1 was prepared according to previous publications with some modifications.[23,24] The regenerated birch wood meal (4 g, cellulosic-rich residue 1) was subjected to enzymatic hydrolysis, with the loading of 2.0 mL of cellulase (Celluclast 1.5 L) and 1.0 mL of β-glucosidase (Novozyme 188) in 0.05 M acetate buffer (pH 4.8). The substrate concentration was 2% (200 mL buffer solution). The reaction mixture was incubated at 50 °C in a rotary shaker (150 rpm) for 48 h. After enzymatic hydrolysis, the mixed solution was centrifuged and the enzymatic hydrolysis residue (EHR) was extensively washed with hot water and then freeze-dried. Subsequently, the EHR was extracted with 96% dioxane/water containing 0.05 M hydrochloric acid at 86 °C for 2 h under N₂ protection. After that, the extracting solution was filtered and concentrated and then poured into 10 volumes of distilled water to

precipitate RL preparation. The crude RL was obtained by freeze-drying. CEL was isolated according to the method of Chang et al. with minor modifications.[4] Specifically, milled birch wood (5 g) was subjected to enzymatic hydrolysis as described above and then extracted with 96% aqueous dioxane for 48 h (2 × 24, fresh solvent) at room temperature. After extraction, the extraction solution was filtered and concentrated. The concentrated lignin solution was poured into 10 volumes of acidic water (pH 2) to precipitate the crude CEL preparation. To obtain pure lignin for structural analysis, ILL-1 and ILL-2 were combined and purified by washing with acidic water (pH 2). However, the crude CEL and RL were dissolved in 90% acetic acid and then precipitated into 10 volumes of distilled water to obtain purified lignin samples. After centrifugation, three purified lignin fractions (ILL, RL, and CEL) were obtained.

Characterization of Lignins. *Associated Polysaccharides Analysis.* The composition of structural carbohydrates was analyzed by high-performance anion exchange chromatography (HPAEC) as reported previously.[26]

FT-IR Analyses. FT-IR spectra of lignin preparations were obtained using a Thermo Scientific Nicolet iN10 FT-IR microscope (Thermo Nicolet Corp., Madison, WI, USA) equipped with a liquid nitrogen cooled MCT detector. The dried lignin samples were ground and pelletized using BaF_2, and their spectra were recorded in the range from 4000 to 700 cm^{-1} at 4 cm^{-1} resolution and 128 scans per sample. The fingerprint region was baseline corrected between 1900 and 750 cm^{-1}.

GPC Analyses. The weight-average (M_w) and number-average (M_n) molecular weights of the acetylated lignin preparations were determined by GPC with an ultraviolet detector (UV) at 240 nm.[27] The column used was a PL-gel 10 mm mixed-B 7.5 mm i.d. column, which was calibrated with PL polystyrene standards. Four milligrams of acetylated lignin was dissolved in 2 mL of tetrahydrofuran (THF), and 20 μL lignin solutions were injected. The column was operated at ambient temperature and eluted with THF at a flow rate of 1.0 mL/min.

NMR Spectra of the Lignin Fractions. NMR spectra were recorded on a Bruker AVIII 400 MHz spectrometer at 25 °C in DMSO-d_6. For the quantitative ^{13}C NMR experiments, 140 mg of lignin was dissolved in 0.5 mL of DMSO-d_6, and 20 μL of chromium(III) acetylacetonate (0.01 M) was added as a relaxation agent for the quantitative ^{13}C spectrum to reduce the relaxation delay according to a previous paper.[9] The quantitative ^{13}C NMR spectra were recorded in the FT mode at 100.6 MHz. The inverse gated decoupling sequence (C13IG sequence from Bruker Standard Library), which allows quantitative analysis and comparison of signal intensities, was used with the following parameters: 30° pulse angle; 1.4 s acquisition time; 2 s relaxation delay; 64K data points; and 30000 scans. For quantitative 2D-HSQC spectra, the Bruker standard pulse program hsqcetgpsi2 was used for HSQC experiments. ^{31}P NMR spectra were acquired after the reaction of lignin with 2-chloro-1,3,2 dioxaphospholanyl chlorides according to the literature with minor modifications.[28] Especially, 20 mg lignin was dissolved in 500 μL of anhydrous pyridine and deuterated chloroform (1.6:1, v/v) under stirring. This was followed by the addition 100 μL of cyclohexanol (10.85 mg/mL) as an internal standard and 100 μL of chromium(III) acetylacetonate solution (5 mg/mL in anhydrous pyridine and deuterated chloroform 1.6:1, v/v) as relaxation reagent. Finally, the mixture was reacted with 100 μL of phosphitylating reagent (2-chloro-1,3,2-dioxaphospholane) for about 10 min and was transferred into a 5 mm NMR tube for subsequent NMR analysis.

Thermogravimetric Analysis (TGA). Thermal analysis was performed using TGA on a thermal analyzer (The Discovery TGA, TA Instruments). The sample was heated from room temperature to 600 °C at a rate of 10 °C/min in nitrogen.

■ RESULTS AND DISCUSSION

Composition Analysis, Yield, and Associated Neutral Sugars. The compositional analysis of original and IL pretreated birch wood was applied to estimate the effect of IL pretreatment on the composition of birch wood, and the

results are summarized in Table 1. The Klason lignin content in the original birch was 23.4% (w/w). The carbohydrate analysis

Table 1. Chemical Composition of the Original and IL Pretreated Birch Wood

compound	original birch (%)	pretreated birch (%)
glucan	35.0	52.5
xylan	20.7	12.8
arabinan	0.47	tr[a]
mannan	7.49	tr
galactan	1.30	tr
Klason lignin	23.4	17.0
acid-soluble lignin	2.00	3.50

[a]tr, trace amount.

revealed that xylan and glucan were the dominant constituents in the original birch, whereas arabinan and mannan were present in only small quantities. After IL pretreatment, the Klason lignin content was decreased to 17.0% (based on pretreated birch). In addition, the relative content of glucan in the pretreated biomass was sharply increased to 52.5%, whereas the relative content of xylan was decreased to ~12.8%. However, the total chemical composition was only 85%, which was still lower than theoretical value, probably due to the existence of some degraded carbohydrates in the pretreated birch. In addition, IL became dark after the recycle, and this was probably due to the degradation of lignin and carbohydrate after the IL pretreatment. However, the subsequent NMR spectrum of the recycled IL was similar to that of fresh IL (spectra not shown). This suggested that the degradation products could not be directly detected by NMR in mixture IL, unless they were extracted with organic solvent (e.g., dichloroethane) from recycled IL. However, the current study was mainly focused on the quantitative structures and thermal properties of the collected lignin fractions after the IL pretreatment; the degradation products in the reclaimed IL will be investigated in the future.

The yields of ILL, RL, and CEL were 26.0, 17.4, and 30.0% of the Klason lignin, respectively (Table 2). A previous study

Table 2. Yield and Carbohydrate Contents of Lignin Preparations

sample	yield[a] (%)	carbohydrate (%)	Ara[b]	Gal[b]	Glu[b]	Xyl[b]	Man[b]
ILL	26.0	3.9	0.26	0.58	0.94	2.11	tr[c]
RL	17.4	1.8	tr	0.22	0.98	0.40	0.22
CEL	30.0	4.6	0.88	0.18	1.47	1.80	0.31

[a]Based on Klason lignin (23% for birch wood). [b]Ara, L-arabinose; Gal, L-galactose; Glu, D-glucose; Xyl, D-xylose; Man, D-mannose. [c]tr, trace amount.

showed that the yield of CEL was much higher than the corresponding MWL.[29] In the present study, the total yield of successive lignin fractions collected after the IL pretreatment reached 43.4% based on Klason lignin, which was higher than the corresponding CEL (30%). Therefore, the combined lignin samples could be more representative fractions for investigating the structural changes involved in the IL process. In general, the lignin samples for structural analysis should have a lower content of carbohydrates. Clearly, the lignin fractions collected in this study contained lower levels of associated carbohydrates
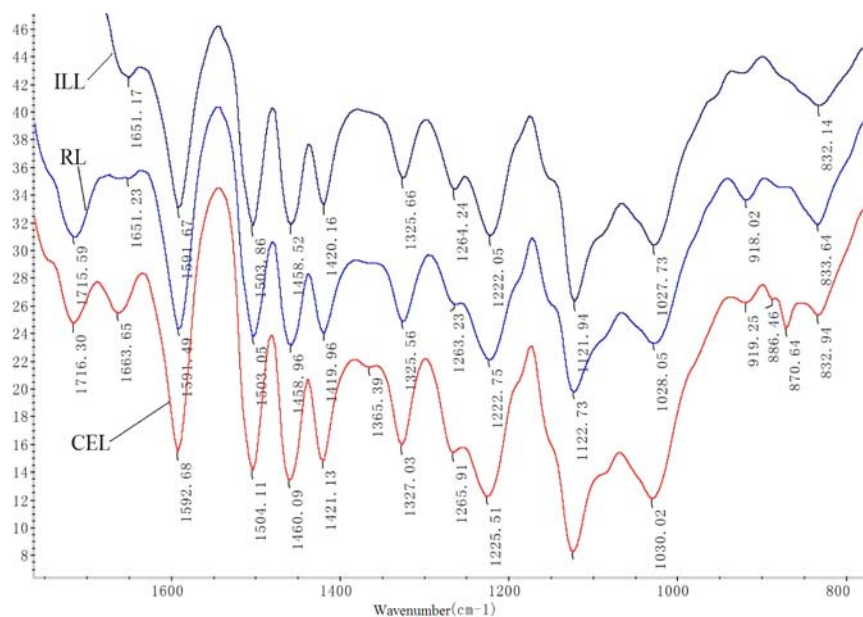
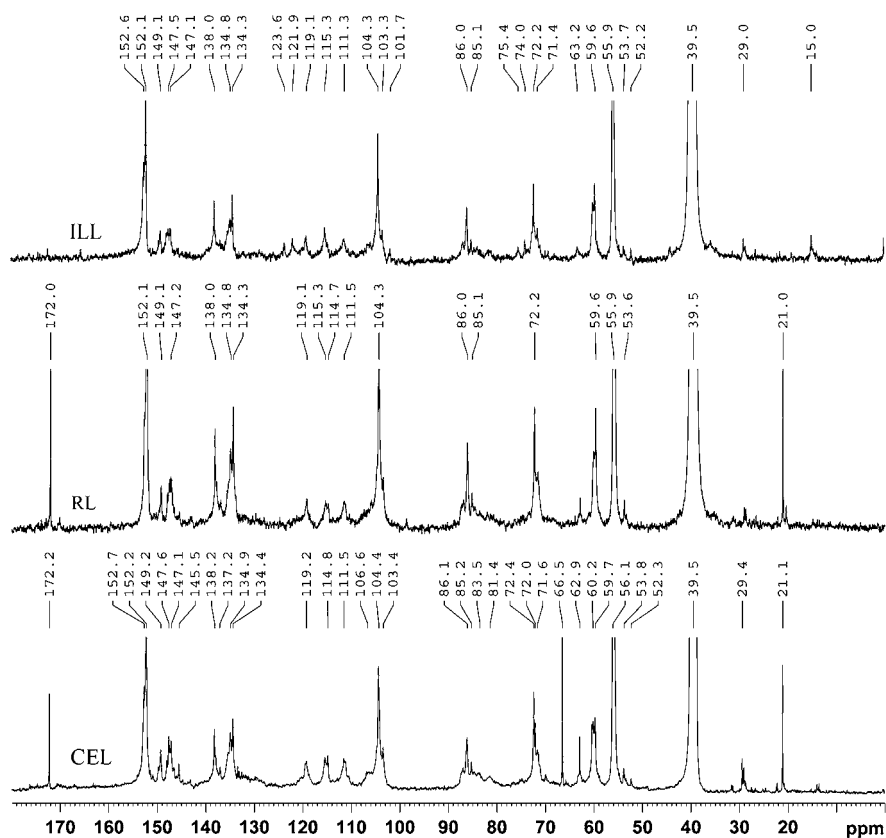**Figure 2.** FT-IR spectra of ILL, RL, and CEL.

Figure 3. Quantitative ^{13}C NMR spectra of ILL, RL, and CEL.

(from 1.8 to 4.6%), as shown in Table 2. Especially, xylose was found to be the major sugar in ILL and CEL, reaching 1.8−2.1% (based on dry lignin), whereas glucose, galactose, and arabinose were observed as noticeable sugars. By contrast, only glucose was found to be the major sugar in RL. The reduced content of xylose in RL suggested that xylans attached to lignin were cleaved after IL pretreatment. In brief, such low contents

of sugar in the lignin samples will be beneficial for subsequent structure analysis.

FT-IR Spectra Analyses. Figure 2 shows the fingerprint region of FT-IR spectra of the lignin samples, and peaks were assigned according to the literature.[30,31] The absorption at 1651−1663 cm^{-1} is attributed to stretching of conjugated C═O groups, which is more pronounced in CEL than in ILL and RL, suggesting that CEL contained more conjugated C═O

groups. In addition, the shift of wavenumber from 1663 to 1651 cm^{-1} in ILL and RL suggested that more electronegative substituents attach to the conjugated lignin units. However, the detailed structures need further confirmation. The bands at 1595, 1506, and 1421 cm^{-1}, corresponding to aromatic skeletal vibrations and the C—H deformation combined with aromatic ring vibration at 1460 cm^{-1}, are presented in Figure 2. The similarity of the spectra suggested that the "core" of the lignin structure did not change significantly after the IL pretreatment. Syringyl and condensed guaiacyl absorptions were obviously observed at 1326 cm^{-1}, whereas guaiacyl ring breathing with C=O stretching appeared at 1264 cm^{-1}. The strong band at 1221 cm^{-1} was ascribed to the C—C, C—O, and C=O stretching. The maximum absorption band at 1120 cm^{-1} was originated from aromatic C—H in-plane deformation (typical for S units). Moreover, additional absorptions appeared at ~1716 cm^{-1} in CEL and RL rather than ILL, suggesting that the existence of more unconjugated C=O units. However, the origin of the unconjugated C=O groups should be confirmed before possible mechanistic pathways are proposed.

Quantitative NMR Spectra. *Quantitative ^{13}C NMR Spectra.* To further understand the structural features of the lignin fractions, the quantitative ^{13}C NMR spectra of the lignins were also recorded as shown in Figure 3. The tiny signals between δ 90 and 102 indicated very low carbohydrate content in these lignin samples, as also revealed by sugar analysis as aforementioned, suggesting that lignin–carbohydrate complex (LCC) structures were partly hydrolyzed after IL pretreatment. It was observed that the spectra of the lignin fractions were very similar except for several peaks. For instance, the signal at 172 and 21 ppm appearing in RL and CEL probably suggested the presence of acetyl groups in acetic acid, which was used to purify the isolated CEL and RL (see Materials and Methods). Subsequent NMR determination of acetic acid (172 and 21 ppm) confirmed that the two signals really resulted from a trace amount of residual acetic acid. Here, the origin of unconjugated C=O groups in lignin samples was also clarified. In addition, the distinct peak at δ 66.5 of CEL probably originated from dioxane.

In the aromatic region (153–103 ppm) of the lignin fractions, the NMR peaks were mostly assigned according to previous publications.[31,32] Syringyl units were detected by signals at δ 152.1 (S-3/5, etherified), δ 147.6 (S-3/5, nonetherified), δ 138.3 (S-4, etherified), δ 134.8 (S-1, etherified), and δ 104.4 (S-2/6). The guaiacyl units give signals at δ 149.1 (G-3, etherified), δ 147.2 (G-4, etherified), δ 134.3 (G-1, etherified), δ 119.1 (G-6), δ 115.3 (G-5), and δ 111.3 (G-2). In addition, *p*-hydroxyphenyl units (H units) were not detected in the current spectra. These observed signals confirmed that the lignin fractions from birch were GS-lignins, in accordance with the FT-IR analysis aforementioned. Furthermore, two additional signals appeared in ILL, located at 121.9 and 123.6 ppm, were tentatively attributed to the presence of oxidized G units (C$_\alpha$=O) or condensed lignin units because the chemical shifts of G-6 will migrate if more conjugated structure occurs at the sidechain of lignin structures or condensed lignin units occur at position 5 of the aromatic ring.

To obtain quantitative information of different structural units in the lignin fractions, quantitative ^{13}C NMR calculation was also applied. The integral values for the structural moieties were reported per aryl groups according to the literature.[10] Table 3 gives the major signal assignments and the quantitative

Table 3. Quantitative Information on the Structures from the Quantitative ^{13}C NMR and 2D-HSQC Spectra of ILL, RL, and CEL^a

δ	assignment	ILL	RL	CEL
160–140	aromatic C—O	2.14	2.17	2.21
140–123	aromatic C—C	1.81	1.72	1.66
123–103	aromatic C—H	2.12	2.20	2.24
61.2–58	β-O-4	0.56 (0.51)	0.59 (0.56)	0.65 (0.58)
58–54	OCH$_3$	1.36	1.66	1.40
54–53	β-β, β-5	0.08	0.07	0.06
	DC^b	0.33	0.25	0.20
	S/G ratio^c	1.14 (1.81)	1.62 (2.72)	1.26 (1.90)

^{a}The data in parentheses were calculated from 2D spectra. S/G = IS$_{2,6}$/2/IG$_2$; the β-O-4 content was calculated on the basis of the literature.[14] ^{b}DC, degree of condensation. s + g + h = 1 (S, G, and H units were calculate from 2D), $I_{theor CAr–H}$= (2s + 3g + 2h), DC = $I_{theor CAr–H}$ − $I_{123–103 ppm}$. ^{c}S/G ratio was calculated from the following formula: S/G = $I_{103–108 ppm}$/$I_{108–114 ppm}$/2.

results of the signals for the lignins. The syringyl/guaiacyl ratio (S/G) was calculated on the basis of the number of carbons per aromatic ring in C2 of guaiacyl and C2/C6 of syringyl units. The integral value between δ 108 and 103 divided by 2 can then estimate the content of syringyl moieties, and the guaiacyl moieties were determined by the integral value between δ 114 and 108. In addition, the S/G ratio was also calculated from 2D-HSQC spectra on the basis of a previous publication.[14] Interestingly, it was found that the ILL contained fewer syringyl units as compared to RL, which was abundant with syringyl units in the current study. By contrast, CEL also contained fewer syringyl units. Cetinkol et al. also observed that IL ([C2 min][OAc]) selectively removed G units lignin fractions and increased the S/G ratio of pretreated wood as compared to original wood.[33] Another previous study reported that the lignin isolated during the early part of ball-milling may originate mainly from lignin in middle lamella,[29] which was reported to contain fewer methoxyl groups per C9 than in the secondary wall lignin.[34] Therefore, a possible speculation is that the lignins with lower S/G ratios were initially extracted, whereas the residual lignins with abundant syringyl units were subsequently extracted, which was probably originated from the secondary wall. The results were in agreement with the data presented in some literatures,[13,35] in which the S/G ratios of the lignins isolated from MWL-pre-extracted wood were increased as compared to that of first-extracted MWL. Similarly, another study also found that alkaline sulfite pulping with anthraquinone and methanol (ASAM) residual lignin from beech wood was also rich in syringyl units.[36] These findings confirmed that syringyl-rich lignin fractions were extracted from biomass in the later period of the separation process. In consideration of the lower yield and lower S/G ratio of CEL in our study, one possibility is that CEL isolated from birch wood in our study is mainly derived from middle lamella.

The aromatic region in the ^{13}C NMR spectrum (δ 160.0–103.0) can be divided into three broad categories: oxygenated aromatic carbons (δ 160.0–140.0), aromatic carbon–carbon structures (δ 140.0–123.0), and aromatic methine carbons (δ 123.0–103.0). The amounts of oxygenated carbons per aryl in ILL, RL, and CEL were found to be 2.14, 2.17, and 2.21, respectively. The result was in agreement with the FT-IR spectra, in which the content of conjugated C=O is higher in CEL as compared to that of ILL and RL. However, the content
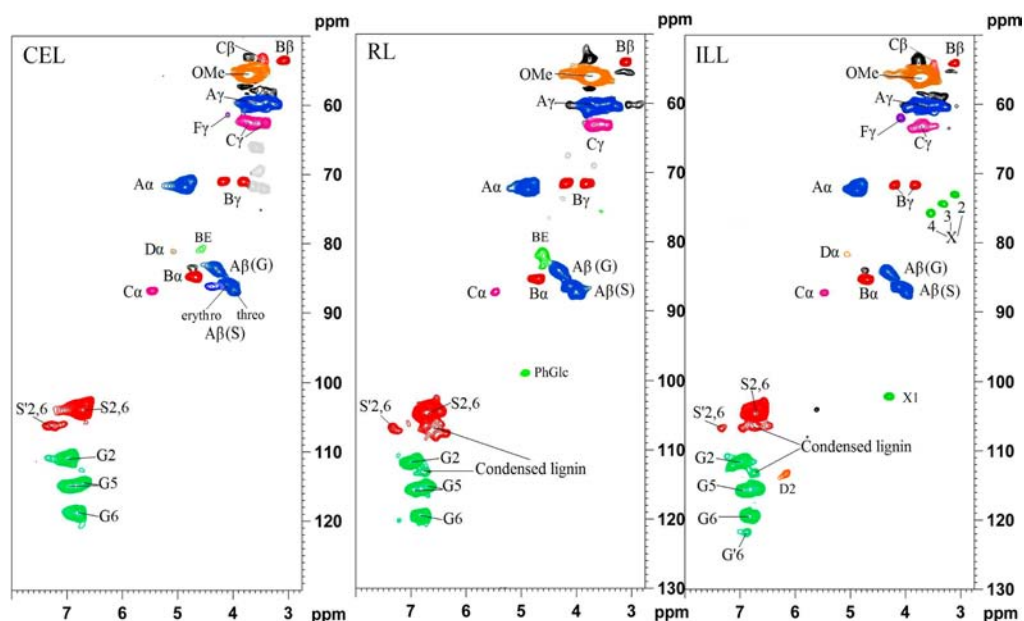
Figure 4. Quantitative 2D-HSQC spectra of ILL, RL, and CEL.

of carbon−carbon structures in ILL was slightly higher than those of RL and CEL as revealed by quantitative ^{13}C NMR spectra. The degree of condensation (DC) was determined by subtracting the observed signal intensity for C_{Ar-H} (δ 123−103) from the theoretical value of C_{Ar-H}.[10] The calculated DC values for ILL, RL, and CEL were 33, 25, and 20%, respectively. The increased DC in ILL was also supported by the increased number of aromatic C−C and the decreased number of aromatic methine carbons as shown in Table 3. In addition, the data clearly showed that the amount of β-O-4 in ILL is slightly lower than those of RL and CEL. This agreed well with the results reported by a recent publication, in which the β-aryl ether linkage of lignin was found to be decreased as a result of IL pretreatment.[22] However, the amounts of β-5 and β-β increased in ILL compared with those of RL and CEL, suggesting that more condensed lignin occurred in ILL. Furthermore, the lower S/G ratio of ILL also added some clues to explain the high content of condensed structure in it because the guaiacyl-type (G) lignin units were found to be reactive toward condensation during the pretreatment.[37]

Quantitative 2D-HSQC Spectra. To obtain more detailed chemical information of the lignin fractions, quantitative 2D-HSQC spectra of the lignins were also acquired. Figure 4 shows the side-chain and aromatic regions of HSQC spectra for the lignins. The obvious correlations, such as those from substructures of β-ether (β-O-4, A), resinol (β-β, B), phenyl-coumaran (β-5, C), and some minor structural units (D, spirodienone; F, p-hydroxycinnamyl alcohol end groups), can be assigned according to the recent literatures and are depicted in Figure 5.[31,38]

Comparison of the 2D-HSQC NMR spectra provides more detail information about the fine structural features of the lignin fractions. No significant differences in the side-chain region of the spectra have been observed. The signals for spirodienone structure (D) presented in ILL and CEL but not in RL suggested that the spirodienone unit (D) was not stable in the acidic conditions as the reaction progressed. Coincidently, similar results were also reported by Hallac et al.[37] when they investigated lignin under acidic condition. In addition, the fact

that related signals of xylans were observed while the signals for acetylated xylans disappeared in ILL suggested that the deacetylation of xylans occurred during the IL pretreatment.

In the region of anomeric carbohydrates, the observed signal at 99.5/4.90 ppm in RL was tentatively assigned to phenyl glycoside linkages (PhGlc) according to model compound data,[39] which suggested that more lignin−carbohydrate linkages could be mainly found in RL. Similarly, the benzyl−ether (BE) linkage was also detected at δ 81.0/4.65 in CEL and RL. The signals appearing for PhGlc and benzyl−ether linkages in RL revealed that more LCC linkages probably occurred in the secondary wall than in middle lamella because RL was originated from the secondary wall. However, another signal, which appeared at 102.0/4.32 ppm in ILL, was attributed to the β-D-xylopyranoside unit, suggesting that xylans were associated with ILL.

In the aromatic regions in the HSQC spectra of the lignins, cross-signals from syringyl (S) and guaiacyl (G) lignin units were distinctly differentiated. However, p-hydroxyphenyl (H) was not observed. The normal S-type lignin units showed a prominent signal for the $C_{2,6}-H_{2,6}$ correlation at δ_C/δ_H 104.2/6.72, whereas the signals corresponding to $C_{2,6}-H_{2,6}$ correlations in C_α-oxidized S units (δ_C/δ_H 106.2/7.27) are also present in the HSQC spectra of the lignin fractions. By contrast, the G units showed different correlations for C_2-H_2, C_5-H_5, and C_6-H_6 at δ_C/δ_H 111.4/6.96, 114.8/6.71 + 6.94, and 119.8/6.72 ppm, respectively. Two observed signals at C-5 were attributed to different substituents at C-4 position. In addition, some condensed lignin structures likely occurred at G_2 and $S_{2,6}$ (Figure 4). The C−H correlations from condensed lignin structures are the 2-position of guaiacyl units linked at the 5-position to other lignin side chains.[22] However, the detailed structures of condensed lignin formed in S units remained unknown. The condensed position in S units is probably located at C_α of the side chain, which can then react with another lignin unit.[40] The migration of chemical shift at G_6 was probably due to the formation of a new carbon−carbon bond by acid-catalyzed condensation because the election-cloud density of G-units aromatic ring increased, which led to the
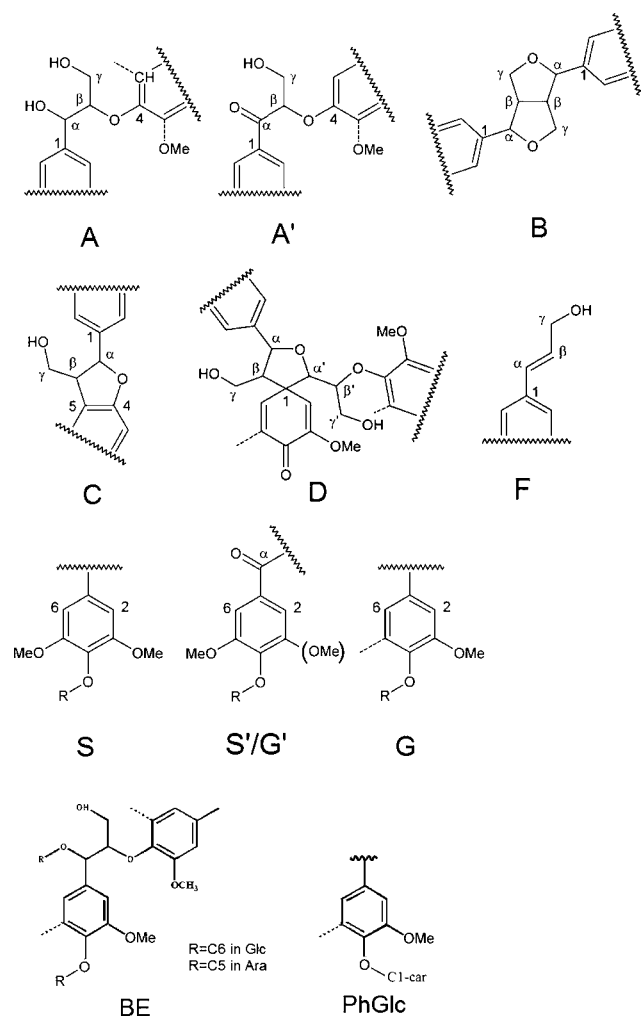
Figure 5. Main classical structures in the lignin preparations (A) β-O-4 linkages; (A′) C$_α$-oxidized β-O-4 linkage substructures; (B) resinol structures formed by β-β/α-O-γ/γ-O-α linkages; (C) phenylcoumarane structures formed by β-5/α-O-4 linkages; (D) spirodienone structures formed by β-1 linkages; (F) p-hydroxycinnamyl alcohol end groups; (G) guaiacyl unit; (G′) oxidized guaiacyl units with a C$_α$ ketone (S) syringyl unit; (S′) oxidized syringyl unit linked a carbonyl or carboxyl group at C$_α$ (phenolic). Possible lignin−carbohydrate linkages: PhGlc, phenyl glycoside; BE, benzyl ether.

obvious shift of other correlations, especially for G$_2$.[41] Similarly, some condensed G$_2$ was observed in some softwood species in a previous publication.[22] In short, the structural features of lignin fractions collected after the IL pretreatment slightly condensed as compared to the corresponding CEL.

31P NMR Analysis of Lignin. The origin and content of hydroxyl groups in lignin could be obtained from ^{31}P NMR spectra. In detail, α-OH (*erythro* and *threo* form) is located at the range of 136.0−135.0 and 134.5−133.8, whereas the primary OH range is from 133.3 to 132 ppm. For aromatic OH groups (S−OH, G$_{5,5}$−OH, and G−OH), the regions of integration are 132−131.5, 131.5−131.0, and 130.3−129.5 ppm, respectively. In addition, the COOH group is calculated on the basis of the range of 128−126 ppm, whereas the internal standard (cyclohexanol) gives a range of 133.8−133.3 ppm, which is between α-OH and primary OH regions.

The ^{31}P NMR data confirmed that original birch lignin belongs to the guaiacyl−syringyl type, as evidenced by the presence of syringyl- and guaiacyl-type phenolic structures in

the ^{31}P NMR spectra of all lignin samples (Table 4). The decrease of aliphatic hydroxyl groups in ILL could be attributed

Table 4. Functional Groups of Lignins As Determined by Quantitative ^{31}P NMR (Millimoles per Gram)

functional group	ILL	RL	CEL
α-OH (*erythro*)	0.86	1.20	0.92
α-OH (*threo*)	0.48	0.66	0.52
primary OH	3.05	4.40	3.48
S−OH	0.54	0.47	0.44
G$_{5,5}$−OH	0.23	0.23	0.15
G−OH	0.60	0.48	0.44
COOH	0.37	0.33	0.08

to the dehydration reaction and acid-catalyzed elimination reactions occurring during ILL pretreatment, as also reported by another study.[42] The IL pretreatment resulted in an increase of phenolic hydroxyl, which also corresponded to the low molecular weight and low β-O-4 content of ILL. The contents of carboxyl OH groups were found to be 0.37 and 0.25 mmol/g for ILL and RL, respectively, which were higher than that of corresponding CEL (0.08 mmol/g), suggesting that the IL pretreatment resulted in an increase of carboxyl OH groups. The increased carboxyl OH suggested that oxidation of aliphatic OH has occurred during the IL pretreatment process.

Molecular Weight Determination. To investigate the effect of IL pretreatment on the molecular weights of lignin samples, GPC analysis of the lignin samples was performed. Figure 6 depicts the average molecular weights (M_w) and the polydispersity index (PI) (M_w/M_n) of the lignins. As compared with the M_w and PI of CEL, ILL and RL exhibited significant decreases in M_w and PI. The results revealed that IL pretreatment has a significant effect on the molecular weight of lignins, which was probably due to the depolymerization. A recent publication also demonstrated that lignin subunits after pretreatment of [C$_2$mim][OAc] were released via dissociation or depolymerization, thus resulting in the reduced size and shape of lignin.[43,44] Together with the higher content of phenolic OH, the lower M_w value for ILL is good evidence for lignin depolymerization by the IL pretreatment. In addition, the slight increase of phenolic OH in RL as compared to CEL also implied that residual lignin extracted as RL was also somewhat depolymerized under the conditions given. Moreover, IL lignin sample with lower PI indicated that the IL pretreatment resulted in homogeneous lignin fragments with narrow PI ($M_w/M_n = 1.49$−1.62) as compared to that of CEL. Furthermore, the content of β-O-4 is positively related to the M_w of the lignins. Especially, the greater the β-O-4 content, the higher the M_w of the lignin. A similar order was also observed in a recent publication.[31] The amounts of β-O-4 units increased in the order ILL < RL < CEL, indicating that ILL is the most degraded sample, whereas CEL undergoes less degradation.

TGA. To study the relationship between quantitative structure and thermal properties, TGA and quantitative NMR spectra of the lignin fractions were comparatively investigated. In general, the different thermal stabilities are not only influenced by inherent structure and various functional groups of lignin polymers, degree of branching, and condensation of the lignin macromolecule but also related to specific chemical structures.

The maximum decomposition temperature (T_M) was defined in previous literature;[45] it is the corresponding temperature of
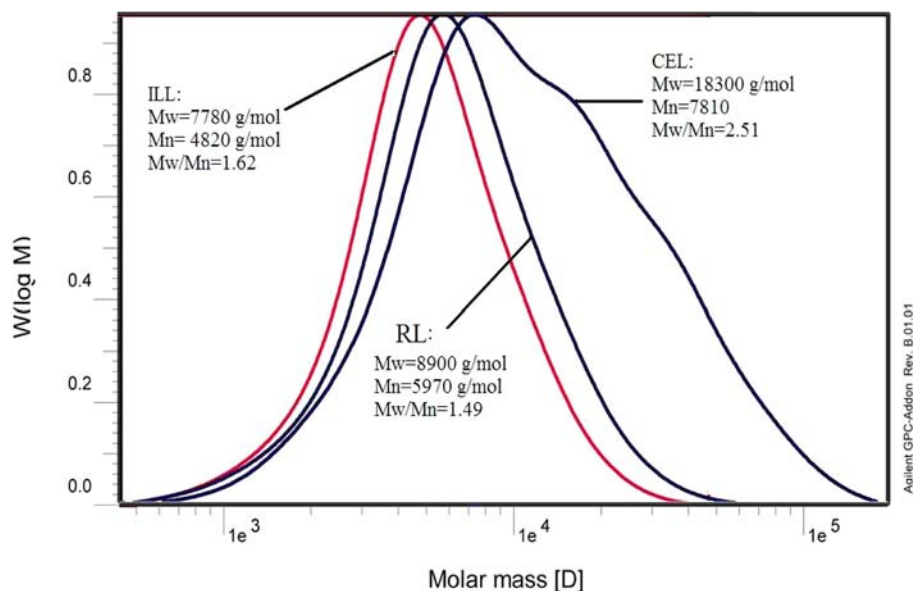
Figure 6. Molecular weight distributions of ILL, RL, and CEL.
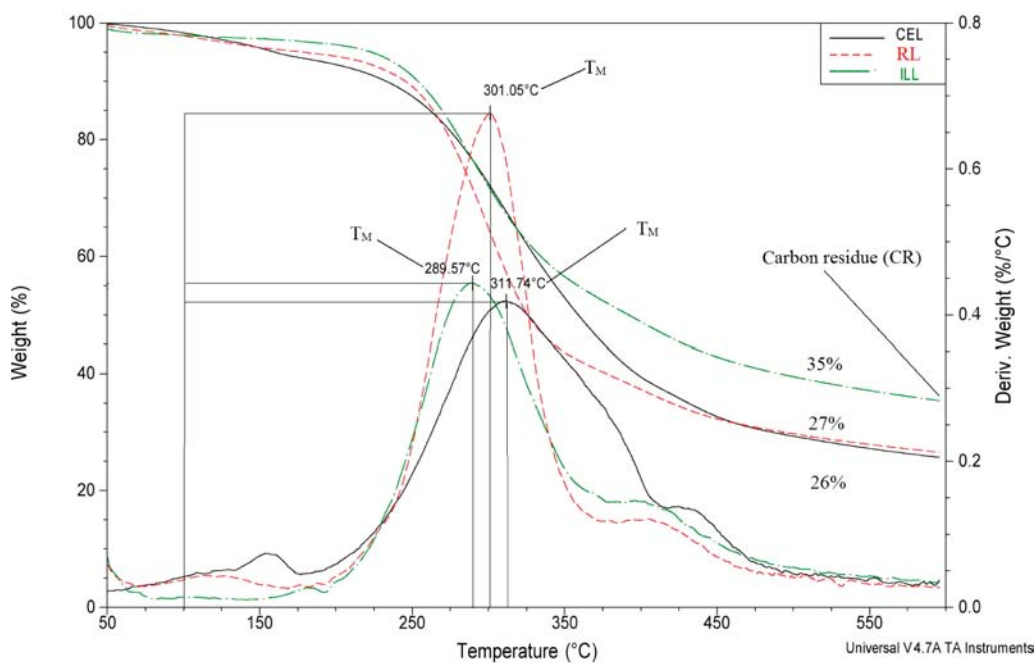

Figure 7. TG/DTG curves of ILL, RL, and CEL.

the maximum decomposition rate (V_M). As shown in Figure 7, it was found that the T_M increased in the order ILL < RL < CEL at the beginning of lignin decomposition (250−350 °C), which was found to be related to the molecular weight, as also revealed by Sun et al.[46] In other words, higher molecular weight leads to a shift of the maximum decomposition temperature (T_M) to a higher temperature region, as also revealed by the data presented here (Figure 7). This is probably because the initial reaction involves the deformation of the weaker C−O bond in the β-O-4 structure during the lignin decomposition.[47] Most of the ether linkages were expected to be cleaved at the stage of 200−350 °C,[47] confirmed by the high content of β-O-4 in the CEL (Table 3). In addition, typical weight losses in TG curves flatten out at temperatures >500 °C, with a slow release of the final products before final char formation. Cracking of

the methoxy (−OCH$_3$) groups released methane around 400−600 °C.[48] It was found that the "char residues" at 600 °C were 26% for CEL, 27% for RL, and 35% for ILL in the present study. This fact suggested that more condensed lignin structures were found in ILL than in CEL and RL, as revealed by the higher DC value obtained from quantitative NMR data (Table 3). In addition, the content of char residue is inversely proportional to the amount of methoxy groups contained in the lignin samples (Table 3), as also reported by other authors.[49] From the above observations, it can be concluded that the lignin having more condensed structures and less content of OCH$_3$ groups resulted in more "char residue". However, lignin with a higher molecular weight and more β-O-4 structures has a higher T_M at the major lignin decomposition.
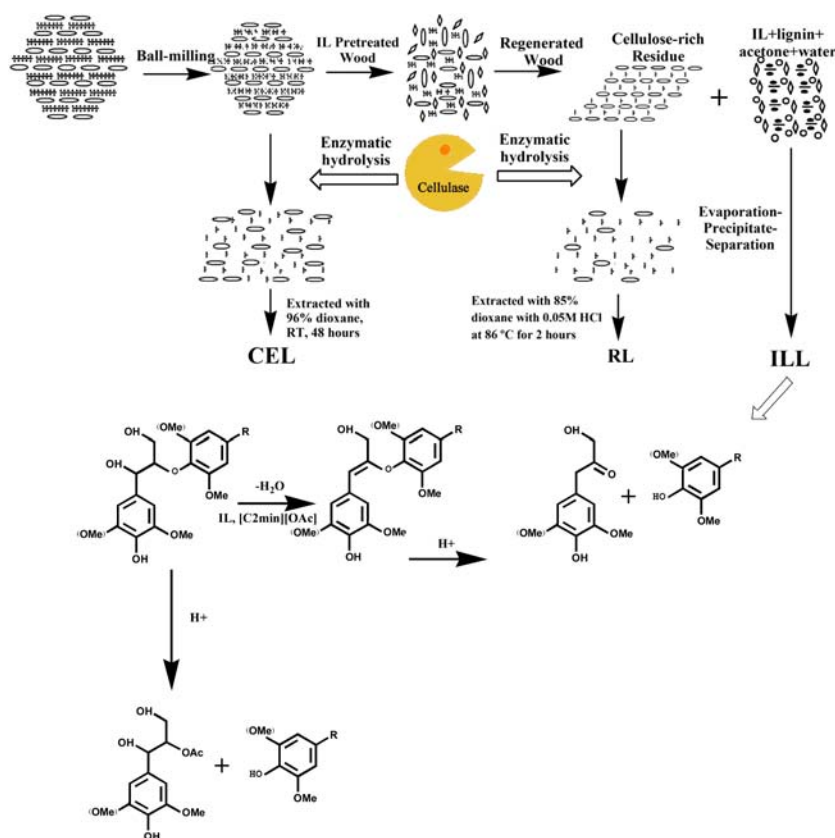
Figure 8. Possible separation mechanism of extracted lignin with ionic liquid.

Possible Separation Mechanism of Lignin after Ionic Liquid Pretreatment. Regardless of the effects of ball-milling on the lignin release for further extraction, here the possible separation mechanisms by ionic liquid are mainly discussed. It is well-known that the extractions of MWL and CEL were mainly based on the theory of "similarity and compatibility". Similarly, the isolation of lignin from ionic liquid also obeys this rule. Evidence to support the separation mechanism of ionic liquid was also presented, which was derived from the present study and the existing studies.[21,22] A previous study showed that the IL pretreatment caused structural modifications to the lignin and polysaccharides that included loss of ether linkages and formation of condensed structures in the lignin from *P. radiata* compression wood by in situ NMR approach.[22] However, the insufficient characterization of IL-induced lignin occurring during the IL pretreatment somewhat impedes the deep and comprehensive understanding of the effects of IL-based pretreatment on the structural features of lignin. In light of our results and previous studies, the possible separation mechanism of lignin during IL pretreatment was proposed as follows. (1) Ball-milled wood was first completely dissolved in the IL ([C_2min][OAc]) because the hydrogen bonds in the biomass were destroyed during IL pretreatment. (2) Dehydration reaction probably occurred in the released lignin fragments; therefore, more conjugated structures occurred in the ILL, and these structures were probably transformed into Hibbert's ketone under acidic condition as the reaction progressed.[50] (3) Lignin−carbohydrate complexes were partially cleaved during the IL pretreatment, probably due to the acidic condition resulting from dehydration reaction. (4) β-O-4 linkages of lignin were also somewhat cleaved during IL pretreatment. (5). After IL pretreatment, the dissolved cell wall components were regenerated by mixed organic solvents; therefore, the released lignin- and cellulose-rich material was separated. A diagram of the proposed separation mechanism is shown in Figure 8.

In conclusion, the present study quantitatively investigated the structural features of lignins collected after an IL pretreatment process. The comprehensive analysis of sequential lignin samples provided insights into how lignin structure changes upon IL pretreatment. A significant decrease in the molecular weight of ILL and RL after IL pretreatment suggested that the homolytic cleavage of β-O-4 interlinkages has occurred, as indicated by the quantitative ^{13}C, 2D-HSQC, and ^{31}P NMR methodologies. Additionally, the suggested separation mechanism of ILL could also account for the structural characteristics and decreased molecular weights of ILL. Moreover, a possible relationship between quantitative structures and thermal properties was found; that is, higher molecular weight and higher β-O-4 content will lead to a higher T_M at the major lignin decomposition stage, whereas more condensed lignin structures in ILL than in RL and CEL provide evidence of higher content of "carbon residue" remaining in ILL than in CEL and RL. However, typical lignin structural features in the original lignin (CEL), such as β-O-4, β-β, and β-5 linkages, are mostly preserved in the lignins isolated after IL pretreatment, although some cleavage and condensation occur after the IL pretreatment process. In view of the typical structural units and thermal properties of the lignins, consequently, this would also make easier the further utilization of these lignins as starting materials for high-value-added products.

■ ASSOCIATED CONTENT

S Supporting Information

Additional table. This material is available free of charge via the Internet at http://pubs.acs.org.

■ AUTHOR INFORMATION

Corresponding Author

*Phone: +86-10-62336903. Fax: +86-10-62336903. E-mail: rcsun3@bjfu.edu.cn.

Notes

The authors declare no competing financial interest.

■ REFERENCES

(1) Ralph, J.; Bunzel, M.; Marita, J. M.; Hatfield, R. D.; Lu, F.; Kim, H.; Schatz, P. F.; Grabber, J. H.; Steinhart, H. Peroxidase-dependent cross-linking reactions of phydroxycinnamates in plant cell walls. *Phytochem. Rev.* **2004**, *3*, 79−96.

(2) Yaku, F.; Tanaka, R.; Koshijima, T. Lignin carbohydrate complex. Part. IV. Lignin as side chain of the carbohydrate in Bjorkman LCC. *Holzforschung* **1981**, *35*, 177−181.

(3) Björkman, A. Isolation of lignin from finely divided wood with neutral solvents. *Nature* **1954**, *174*, 1057−1058.

(4) Chang, H. M.; Cowling, E. B.; Brown, W.; Adler, E.; Miksche, G. Comparative studies on cellulolytic enzyme lignin and milled wood lignin of sweetgum and spruce. *Holzforschung* **1975**, *29*, 153−159.

(5) Wu, S. B.; Argyropoulos, D. S. An improved method for isolating lignin in high yield and purity. *J. Pulp Pap. Sci.* **2003**, *29* (7), 235−240.

(6) Freidenberg, K.; Lautsch, W.; Engler, K. Die Bildung von Vanillin aus Fichten lignin. *Ber. Dtsch. Chem. Ges. A/B* **1940**, *73*, 167−171.

(7) Lapierre, B.; Monties, B.; Rolando, C. Thioacidolysis of lignin: comparison with acidolysis. *J. Wood Chem. Technol.* **1985**, *5* (2), 277−292.

(8) Lu, F. C.; Ralph, J. DFRC method for lignin analysis. 1. New method for α-aryl ether cleavage: lignin model studies. *J. Agric. Food Chem.* **1997**, *45*, 4655−4660.

(9) Capanema, E. A.; Balakshin, M. Y.; Kadla, J. F. A comprehensive approach for quantitative lignin characterization by NMR spectroscopy. *J. Agric. Food Chem.* **2004**, *52*, 1850−1860.

(10) Capanema, E. A.; Balakshin, M. Y.; Kadla, J. F. Quantitative characterization of a hardwood milled wood lignin by nuclear magnetic resonance spectroscopy. *J. Agric. Food Chem.* **2005**, *53*, 9639−9649.

(11) Holtman, K. M.; Chang, H. M.; Jameel, H.; Kadla, J. F. Quantitative ^{13}C NMR characterization of milled wood lignins isolated by different milling techniques. *J. Wood Chem. Technol.* **2006**, *26*, 21−34.

(12) Balakshin, M.; Capanema, E.; Gracz, H.; Chang, H. M.; Jameel., H. Quantification of lignin−carbohydrate linkages with high-resolution NMR spectroscopy. *Planta* **2011**, *233*, 1097−1110.

(13) Yuan, T. Q.; Sun, S. N.; Xu, F.; Sun, R. C. Characterization of lignin structures and lignin-carbohydrate complex (LCC) linkages by quantitative C-13 and 2D HSQC NMR spectroscopy. *J. Agric. Food Chem.* **2011**, *59*, 10604−10614.

(14) Sette, M.; Wechselberger, R.; Crestini, C. Elucidation of lignin structure by quantitative 2D NMR. *Chem.−Eur. J.* **2011**, *17*, 9529−9535.

(15) Mäki-Arvela, P.; Anugwom, I.; Virtanen, P.; Sjöholm, R.; Mikkola, J. P. Dissolution of lignocellulosic materials and its constituents using ionic liquids − a review. *Ind. Crops Prod.* **2010**, *32*, 175−201.

(16) Sun, N.; Rahman, M.; Qin, Y.; Maxim, M. L.; Rodriguez, H.; Rogers, R. D. Complete dissolution and partial delignification of wood in the ionic liquid 1-ethyl-3-methylimidazolium acetate. *Green Chem.* **2009**, *11*, 646−655.

(17) Lee, S. H.; Doherty, T. V.; Linhardt, R. J.; Dordick, J. S. Ionic liquid-mediated selective extraction of lignin from wood leading to enhanced enzymatic cellulose hydrolysis. *Biotechnol. Bioeng.* **2009**, *102*, 1368−1376.

(18) Klein-Marcuschamer, D.; Simmons, B. A.; Blanch, H. W. Technoeconomic analysis of a lignocellulosic ethanol biorefinery with ionic liquid pretreatment. *Biofuels Bioprod. Biorefin.* **2011**, *5* (5), 562−569.

(19) Arora, R.; Manisseri, C.; Li, C. L.; Ong, M. D.; Scheller, H. V.; Vogel, K.; Simmons, B. A.; Singh, S. Monitoring and analyzing process streams towards understanding ionic liquid pretreatment of switchgrass (*Panicum virgatum* L.). *BioEnergy Res.* **2010**, *3*, 134−145.

(20) Li, C. L.; Knierim, B.; Manisseri, C.; Arora, R.; Scheller, H. V.; Auer, M.; Vogel, K. P.; Simmons, B. A.; Singh, S. Comparison of dilute acid and ionic liquid pretreatment of switchgrass: biomass recalcitrance, delignification and enzymatic saccharification. *Bioresour. Technol.* **2010**, *101*, 4900−4906.

(21) Kim, J. Y.; Shin, E. J.; Eom, I. Y.; Won, K.; Kim, Y. H.; Choi, D.; Choi, I. G.; Choi, J. W. Structural features of lignin macromolecules extracted with ionic liquid from poplar wood. *Bioresour. Technol.* **2011**, *102*, 9020−9025.

(22) Torr, K. M.; Love, K. T.; Cetinkol, O. P.; Donaldson, L. A.; George, A.; Holmes, B. M.; Simmons, B. A. The impact of ionic liquid pretreatment on the chemistry and enzymatic digestibility of *Pinus radiata* compression wood. *Green Chem.* **2012**, *14*, 778−787.

(23) Jaaskelainen, A. S.; Sun, Y.; Argyropoulos, D. S.; Tamminen, T.; Hortling, B. The effect of isolation method on the chemical structure of residual lignin. *Wood Sci. Technol.* **2003**, *37*, 91−102.

(24) Argyropoulos, D. S.; Sun, Y.; Paluš, E. Isolation of residual kraft lignin in high yield and purity. *J. Pulp Pap. Sci.* **2002**, *28*, 50−54.

(25) Sluiter, A.; Hames, B.; Ruiz, R.; Scarlata, C.; Sluiter, J.; Templeton, D.; Crocker, D. *Determination of Structural Carbohydrates and Lignin in Biomass*; Technical Report NREL/TP-510-42618, 2008.

(26) Wen, J. L.; Sun, Z. J.; Sun, Y. C.; Sun, S. N.; Xu, F.; Sun, R. C. Structural characterization of alkali-extractable lignin fractions from bamboo. *J. Biobased Mater. Bioenergy* **2010**, *4*, 408−425.

(27) Salanti, A.; Zoia, L.; Tolppa, E. L.; Orlandi, M. Chromatographic detection of lignin-carbohydrate complexes in annual plants by derivatization in ionic liquid. *Biomacromolecules* **2012**, *13*, 445−454.

(28) Faix, O.; Argyropoulos, D. S.; Robert, D.; Neirinck, V. Determination of hydroxyl groups in lignins evaluation of ^{1}H-, ^{13}C-, and ^{31}P-NMR FT-IR and wet chemical methods. *Holzforschung* **1994**, *48*, 387−394.

(29) Hu, Z. J.; Yeh, T. F.; Chang, H. M.; Matsumoto, Y.; Kadla, J. F. Elucidation of the structure of celluloytic enzyme lignin. *Holzforschung* **2006**, *60*, 389−397.

(30) Faix, O. Classification of lignins from different botanical origins by FT-IR spectroscopy. *Holzforschung* **1991**, *45*, 21−27.

(31) Wen, J. L.; Xue, B. L.; Xu, F.; Sun, R. C. Unmasking the structural features and property of lignin from bamboo. *Ind. Crops Prod.* **2013**, *42*, 332−343.

(32) Nimz, H. H.; Robert, D.; Faix, O.; Nemr, M. Carbon-13 NMR spectra of lignins, 8*: structural differences between lignins of hardwood, softwoods, grasses and compression wood. *Holzforschung* **1981**, *35*, 16−26.

(33) Cetinkol, Ö. P.; Dibble, D. C.; Cheng, G.; Kent, M. S.; Knierim, B.; Auer, M.; Wemmer, D. E.; Pelton, J. G.; Melnichenko, Y. B.; Ralph, J.; Simmons, B. A.; Holmes, B. M. Understanding the impact of ionic liquid pretreatment on eucalyptus. *Biofuels* **2009**, *1* (1), 33−46.

(34) Whiting, P.; Goring, D. A. I. Chemical characterization of tissue fractions from the middle lamella and secondary wall of black spruce tracheids. *Wood Sci. Technol.* **1982**, *16*, 261−267.

(35) Yuan, T. Q.; Sun, S. N.; Xu, F.; Sun, R. C. Structural characterization of lignin from triploid of *Populus tomentosa* Carr. *J. Agric. Food Chem.* **2011**, *59* (12), 6605−6615.

(36) Choi, J. W.; Faix, O. NMR study on residual lignins isolated from chemical pulps of beech wood by enzymatic hydrolysis. *J. Ind. Eng. Chem.* **2011**, *17*, 25−28.

(37) Hallac, B. B.; Pu, Y. Q.; Ragauskas, A. J. Chemical transformations of *Buddleja davidii* lignin during ethanol organosolv pretreatment. *Energy Fuels* **2010**, *24*, 2723−2732.

(38) Rencoret, J.; del Rio, J. C.; Gutierrez, A.; Martinez, A. T.; Li, S. M.; Parkas, J.; Lundquist, K. Origin of the acetylated structures present in white birch (*Betula pendula* Roth) milled wood lignin. *Wood Sci. Technol.* **2012**, *46*, 459−471.

(39) Terashima, N.; Ralph, S. A.; Landucci, L. L. New facile synthesis of monolignol glycosides, *p*-glucocoumaryl alcohol, coniferin and syringin. *Holzforschung* **1996**, *50*, 151−155.

(40) Li, J.; Henriksson, G.; Gellerstedt, G. Lignin depolymerization/ repolymerization and its critical role for delignification of aspen wood by steam explosion. *Bioresour. Technol.* **2007**, *98*, 3061−3068.

(41) Wang, K.; Yang, H. Y.; Yao, X.; Xu, F.; Sun, R. C. Structural transformation of hemicelluloses and lignin from triploid poplar during acid-pretreatment based biorefinery process. *Bioresour. Technol.* **2012**, *116*, 99−106.

(42) El Hage, R.; Brosse, N.; Chrusciel, L.; Sanchez, C.; Sannigrahi, P.; Ragauskas, A. Characterization of milled wood lignin and ethanol organosolv lignin from miscanthus. *Polym. Degrad. Stab.* **2009**, *94*, 1632−1638.

(43) Cheng, G.; Kent, M. S.; He, L.; Varanasi, P.; Dibble, D.; Arora, R.; Deng, K.; Hong, K.; Melnichenko, Y. B.; Simmons, B. A.; Singh, S. Effect of ionic liquid treatment on the structures of lignins in solutions: molecular subunits released from lignin. *Langmuir* **2012**, *28*, 11850− 11857.

(44) George, A.; Tran, K.; Morgan, T. J.; Benke, P. I.; Berrueco, C.; Lorente, E.; Wu, B. C.; Keasling, J. D.; Simmons, B. A.; Holmes, B. M. The effect of ionic liquid cation and anion combinations on the macromolecular structure of lignins. *Green Chem.* **2011**, *13*, 3375− 3385.

(45) Hodgson, E.; Nowakowski, D.; Shield, I.; Riche, A.; Bridgwater, A. V.; Clifton-Brown, J. C.; Donnison, I. S. Variation in *miscanthus* chemical composition and implications for conversion by pyrolysis and thermo-chemical biorefining for fuels and chemicals. *Bioresour. Technol.* **2011**, *102*, 3411−3418.

(46) Sun, R.; Tomkinson, J.; Lloyd, J. G. Fractional characterization of ash-AQ lignin by successive extraction with organic solvents from oil palm EFB fibre. *Polym. Degrad. Stab.* **2000**, *68*, 111−119.

(47) Faravelli, T.; Frassoldati, A.; Migliavacca, G.; Ranzi, E. Detailed kinetic modeling of the thermal degradation of lignins. *Biomass Bioenerg.* **2010**, *34*, 290−301.

(48) Yang, H.; Yan, R.; Chen, H.; Lee, D. H.; Zheng, C. Characteristics of hemicelluloses, cellulose and lignin pyrolysis. *Fuel* **2007**, *86*, 1781−1788.

(49) Jakab, E.; Faix, O.; Tilla, F. Thermal decomposition of milled wood lignins studied by thermogravimetry/mass spectrometry. *J. Anal. Appl. Pyrol.* **1997**, *40−41*, 171−186.

(50) Kubo, S.; Hashida, K.; Yamada, T.; Hishiyama, S.; Magara, K.; Kishino, M.; Ohno, H.; Hosoya, S. A characteristic reaction of lignin in ionic liquids: Glycerol type enol-ether as the primary decomposition product of β-O-4 model compound. *J. Wood Chem. Technol.* **2008**, *28*, 84−96.